# Light-Induced Conformational Change and Transient Dissociation Reaction of the BLUF Photoreceptor Synechocystis PixD (Slr1694).

AUTHOR(S):

Tanaka, Keisuke; Nakasone, Yusuke; Okajima, Koji; Ikeuchi, Masahiko; Tokutomi, Satoru; Terazima, Masahide

CITATION:

Tanaka, Keisuke ...[et al]. Light-Induced Conformational Change and Transient Dissociation Reaction of the BLUF Photoreceptor Synechocystis PixD (Slr1694).. Journal of molecular biology 2011, 409(5): 773-785

ISSUE DATE:

2011-06-24

URL:

http://hdl.handle.net/2433/142947

# Light-Induced Conformational Change and Transient Dissociation Reaction of the BLUF Photoreceptor *Synechocystis* PixD (Slr1694)

Keisuke Tanaka[1], Yusuke Nakasone[1], Koji Okajima[2,3], Masahiko Ikeuchi[2], Satoru Tokutomi[3], and Masahide Terazima[1*]

[1]*Department of Chemistry, Graduate School of Science, Kyoto University, Kyoto 606-8502, Japan*

[2]*Department of Life Sciences (Biology), Graduate School of Arts and Sciences, The University of Tokyo, Meguro, Tokyo 153-8902, Japan*

[3]*Department of Biological Science, Graduate School of Science, Osaka Prefecture University, Sakai, Osaka 599-8531, Japan*

**Corresponding author*: mterazima@kuchem.kyoto-u.ac.jp

Tel/FAX: +81-75-753-4026

*Running title*: Light-induced reaction dynamics of *Synechocystis* PixD

Abbreviations: BLUF, blue light photoreceptor using FAD; TG, transient grating; SEC, size exclusion chromatography.

## Abstract

The light-induced reaction of a BLUF photoreceptor PixD from *Synechocystis* sp. PCC6803 (Slr1694) was investigated using the time-resolved transient grating (TG) method. A conformational change coupled with a volume contraction of 13 mL $mol^{-1}$ was observed with a time constant of 45 ms following photoexcitation. At a weak excitation light intensity, there were no further changes in the volume and the diffusion coefficient (*D*). The determined *D*-value ($3.7 \times 10^{-11}$ $m^2$ $s^{-1}$) suggests that PixD exists as a decamer in solution, and this oligomeric state was confirmed by size exclusion chromatography (SEC) and blue native-polyacrylamide gel electrophoresis. Surprisingly, by increasing the excitation laser power, a large increase in *D* with a time constant of 350 ms was observed following the volume contraction reaction. The *D*-value of this photoproduct species ($7.5 \times 10^{-11}$ $m^2$ $s^{-1}$) is close to that of the PixD dimer. Combined with TG and SEC measurements under light-illuminated conditions, the light-induced increase in *D* was attributed to a transient dissociation reaction of the PixD decamer to a dimer. For the M93A-mutated PixD, no volume or *D*-change was observed. Furthermore, we showed that the M93A mutant did not form the decamer but only the dimer in the dark state. These results indicate that the formation of the decamer and the conformational change around the Met residue are important factors that control regulation of the downstream signal transduction by the PixD photoreceptor.

*Keywords*: photoreceptor; BLUF; dynamics; diffusion; transient grating

## Introduction

Light energy is essential for all kingdoms of life to survive, such that species have acquired various types of strategies to respond to the light environment by use of photoreceptor proteins. BLUF (blue light sensors using a flavin chromophore) is a new class of photoreceptor domains found in bacteria and eukaryotes[1,2]. PixD is cyanobacterial BLUF protein from *Synechocystis* sp. PCC6803 (Slr1694) and *Thermosynechococcus elongatus* BP-1 (Tll0078)[3]. According to the crystal structure, PixD consists of the BLUF domain and additional helices. The most striking characteristic of PixD is the unique formation of oligomers. PixD was found to crystallize to form a decamer in the asymmetric unit with two pentameric rings[4,5]. This decameric structure may play an important role in the signal transduction of PixD proteins. We previously showed that *T. elongatus* PixD (TePixD, Tll0078) maintains a decamer or pentamer form depending on the protein concentration, and only the decamer exhibits a significant conformational change[6]. Since no signal output domain was identified in the amino acid sequences, signal transduction could be mediated by a direct protein–protein interaction. Recently, it was reported that *Synechocystis* PixD (PixD, Slr1694), which regulates phototactic movement of the cyanobacterial cell, also forms a decamer in the presence of the response regulator PixE ($PixD_{10}$–$PixE_5$ complex) in solution in the dark state[7]. The complex was found to disassemble into a PixD dimer and the PixE monomer upon blue light irradiation[7]. To understand the molecular mechanism of the light signal transduction of PixD, the photochemical reaction dynamics, including the changes in the protein conformation and/or interprotein interactions, should be clarified.

The primary event after photon absorption of the PixD proteins is the rearrangement of a hydrogen bonding network in the vicinity of flavin, which is characterized by a ~10 nm red shift of the UV/Vis absorption spectrum[8–10]. Transient absorption studies of PixD showed electron and proton transfers between the Tyr residue and the chromophore within 100 ps after photoexcitation, resulting in the generation of the red-shifted signaling state[11,12]. Fukushima *et al.* compared the absorption spectral change of two PixD proteins at various temperatures and found that both PixD proteins shared a common photocycle despite the low sequence homology[13]. We studied the subsequent reaction dynamics of TePixD using the time-resolved transient grating (TG) method. Two spectrally silent reaction phases with time constants of 40 μs and 4 ms were observed as the expansion of the partial molar volume and a change in the diffusion coefficient ($D$) of the TePixD decamer, respectively[6].

For PixD, AppA, or BlrP1 BLUF domains the structural changes following the primary photoreaction of flavin were found to involve conformation changes of the β5-strand and the

adjacent loop through the motion of the conserved Met and Trp with a variety of experimental techniques such as FTIR, fluorescence, crystallographic, and solution NMR studies[10,14–21]. Furthermore, Masuda *et al.* demonstrated that the Met residue conserved among all BLUF domains plays a crucial role in the downstream signal transduction of PixD in *in vitro* and *in vivo*[22].

Two questions to address are whether the photoreaction of PixD (Slr1694) is similar to TePixD after the primary spectral change and if the change in the oligomeric state from decamer to dimer is induced by light without PixE. In this article, we investigated the light-induced reaction dynamics of *Synechocystis* PixD by the TG method, size exclusion chromatography (SEC) and blue native-polyacrylamide gel electrophoresis (BN-PAGE), and found very different features from that observed for TePixD. The conformational change associated with the volume contraction of 13 mL $mol^{-1}$ occurs with a time constant of 45 ms, which is almost 1000 times slower than that of TePixD. No further conformational change was observed at a weak laser power. The determined *D*-value and SEC revealed that PixD could exist as a decamer in solution. However, interestingly, the PixD decamer dissociated to the dimer with a time constant of 350 ms, as observed in the $PixD_{10}$-$PixE_5$ complex, when a strong excitation was applied. This dissociation reaction may represent a template for the previously reported PixD–PixE interaction. Upon mutation of Met93 to Ala, any volume change reaction and *D*-change were not detected and the M93A mutant PixD did not form the decamer. On the basis of these results, the formation of the decamer and the conformational change of the Met93 residue are important features for facilitating the light signal transduction of the PixD photoreceptor.

## Results and discussion

### TG signal at weak excitation light intensity: Light-induced conformational change of PixD

In principle, the TG signal intensity is proportional to the square of light-induced modulation of the refractive index ($\delta n$) produced by the excitation light intensity[6,23–26]. The time profile represents the reaction kinetics as well as the thermal diffusion and molecular diffusion processes. Fig. 1 shows a typical TG signal after photoexcitation of PixD in the buffer solution at a grating wavenumber $q^2 = 4.0 \times 10^{11}$ $m^{-2}$ and a laser power of 0.2 mJ $cm^{-2}$. This laser power was as low as possible to be still able to detect the TG signal with a reasonable signal-to-noise ratio, and we confirmed that further reduction of the light intensity did not change the signal profile. Upon excitation at this low laser power, the TG signal rose

with an instrumental response, and then decayed back to the baseline followed by a slower rise–decay curve. The decay rate constant of the initial phase coincided with the thermal grating signal of a calorimetric reference solution (bromocresol purple in water). Thus, the faster decay signal was attributed to the thermal grating component due to the heat release from the excited state of the flavin chromophore. The temporal profile of the thermal grating is expressed by[23,24]:

$$\delta n_{\mathrm{th}}(t) = \delta n_{\mathrm{th}}^{0} \exp(-D_{\mathrm{th}} q^2 t), \qquad (1)$$

where $\delta n_{\mathrm{th}}^{0}$ is the initial refractive index change of the thermal grating, $D_{\mathrm{th}}$ is the thermal diffusivity of the solution, and $q$ is the grating wavenumber.

Following the thermal grating, a rise–decay profile was observed in a longer time range. This time profile could be reproduced with a double exponential function. The assignments of these components were made from the $q^2$ dependence of the rate constants. The TG signals at various $q^2$ are depicted in Fig. 2. It is obvious from this figure that the rate constant of the rise component was rather insensitive to the grating wavenumber ($q$), whereas that of the decay was clearly dependent on $q^2$. This feature indicates that a reaction kinetics is involved in the rise component and the decay component represents a molecular diffusion process. Hence, we may analyze the signal based on a reaction scheme[6,24,26]:

$$\mathrm{R} \xrightarrow{h\nu} \mathrm{I} \xrightarrow{k} \mathrm{P}, \qquad \text{(Reaction 1)}$$

where R, I, P, and $k$ represent the reactant, an initial product (intermediate), a final product, and the rate constant of the transition, respectively. Since only one diffusion component was observed, $D$ does not change during the reaction. Hence, the TG signal after the thermal grating should be expressed as:

$$I_{\mathrm{TG}}(t) = \alpha\left[-(\delta n_{\mathrm{P}} - \delta n_{\mathrm{I}})\exp(-k_r t) + (\delta n_{\mathrm{P}} - \delta n_{\mathrm{R}})\exp(-k_d t)\right]^2, \qquad (2)$$

where $\delta n_{\mathrm{R}}$ (> 0), $\delta n_{\mathrm{I}}$ (> 0), and $\delta n_{\mathrm{P}}$ (> 0) are, respectively, the initial refractive index changes of the reactant, an intermediate, and a product. Furthermore, $k_r$ and $k_d$ are the rate constants of the rise and decay components, respectively, and these rate constants should be given by $k_r = D_1 q^2 + k$ and $k_d = D_1 q^2$ ($D_1$: diffusion coefficient of PixD under this condition (Reaction 1)). Calculated curves based on Eq. (2) are shown in Fig. 2, which reproduce the observed signal very well at all $q^2$-values with pre-exponential factors of $\delta n_{\mathrm{R}} < \delta n_{\mathrm{I}} < \delta n_{\mathrm{P}}$. The relation of $\delta n_{\mathrm{R}} < \delta n_{\mathrm{I}}$ is quite reasonable, because the absorption spectrum of I is red-shifted from the ground state and the refractive index of such species is predicted to be larger than that of the reactant on the basis of the Kramers–Kronig relationship. No spectral change was detected after the creation of the red-shifted species formed within

subnanoseconds, such that the reaction with a rate constant of $k$ should represent a volume change. The relation of $\delta n_I < \delta n_P$ indicates that the volume grating reflects a volume contraction reaction of PixD. The refractive index change due to the volume change may be expressed by[25]:

$$\delta n_{vol} = V(dn/dV)\Delta V \Delta N , \quad (3)$$

where $V(dn/dV)$ is the refractive index change by the volume change and $\Delta N$ is the number density. By comparing $\delta n_P - \delta n_I$ (= $\delta n_{vol}$) with $\delta n_{th}^0$ of the calorimetric reference measured under the same experimental conditions, $\Delta V$ was determined to be $-(13 \pm 6)$ mL mol$^{-1}$. The plots of $k_r$ and $k_d$ against $q^2$ are shown in Fig. 3. These plots were linear as predicted by Eq. (2). The $D$-value of PixD was determined from the slope as $(3.7 \pm 0.3) \times 10^{-11}$ m$^2$ s$^{-1}$. The rate constant of the volume contraction reaction ($k$) was determined from the intercept to be $((45 \pm 10)$ ms$)^{-1}$.

The determined $D$-value of PixD ($3.7 \times 10^{-11}$ m$^2$ s$^{-1}$) is much smaller than that expected from its molecular mass (18 kDa). For example, $D$-values of myoglobin (18 kDa), with a similar molecular size to PixD, are $9–11 \times 10^{-11}$ m$^2$ s$^{-1}$. This observation clearly indicates that PixD exists as an oligomeric form in solution. On the other hand, the $D$-value is comparable to that of the PixD protein from *T. elongatus* (TePixD; $D = 4.9 \times 10^{-11}$ m$^2$ s$^{-1}$) which forms a decamer in solution[6]. Therefore, we concluded that PixD also forms a decamer. This conclusion was supported by the SEC measurement as described later. Hence, the decamer form of PixD undergoes a conformational change accompanied by the volume contraction of 13 mL mol$^{-1}$ with the time constant of 45 ms at the weak excitation intensity.

**TG signal at strong excitation light intensity: The transient dissociation reaction of the PixD decamer into the dimer**

As described in the above section, PixD shows a conformational change with the time constant of 45 ms and this conformational change is accompanied with a volume contraction; however, the $D$-value did not change. This feature is quite different from that reported for TePixD, which showed a volume expansion with a time constant of 40 μs as well as a significant $D$-change (from $4.9 \times 10^{-11}$ to $3.2 \times 10^{-11}$ m$^2$ s$^{-1}$) with a time constant of 4 ms[6]. However, interesting $D$-change dynamics were discovered at stronger light intensities for PixD. The TG signals of PixD at various excitation intensities are shown in Fig. 4. The profile gradually changed with increasing laser power; a new rise–decay component appeared in a longer time range and the rise–decay component observed at the weak laser power was noticeably weaker.

This laser power dependence can be explained by a superposition of the contributions from two different reactions; one is obviously the volume change reaction observed at the weak excitation light intensity (Reaction 1), and the other is a signal that reflects a reaction at a strong light intensity (Reaction 2). As stated in the above section, the pre-exponential factors (refractive index change) of the rise and decay components for the Reaction 1 are negative and positive, respectively. Since the signals from Reactions 1 and 2 are destructively overlapping, the refractive index change of the rise and decay components for the Reaction 2 should be positive and negative, respectively. To analyze the TG signal, we should separate the two contributions in the observed signal:

$$I_{\mathrm{TG}}(t) = \alpha\{\delta n_1(t) + f_d \delta n_2(t)\}^2, \qquad (4)$$

where $\delta n_1(t)$ and $\delta n_2(t)$ are the refractive index changes due to the Reaction 1 (Eq. (1)) and the Reaction 2, respectively, and $f_d$ is a laser power-dependent relative contribution of $\delta n_2(t)$. In order to unambiguously fit the signal, it is important to know the time profile of $\delta n_2(t)$. As such, it was found that the profile did not change further above a laser power of > 10 mJ cm$^{-2}$. Under this strong excitation condition, the contribution of $\delta n_2(t)$ was several hundred fold stronger than $\delta n_1(t)$, and thus the contribution of $\delta n_1(t)$ is negligible. Therefore, the TG signal measured at 10 mJ cm$^{-2}$ is considered to be a pure TG signal representing the Reaction 2 ($\delta n_2(t)$). For assigning the rise and decay components of the signal, the TG signals were measured at higher laser powers (>10 mJ cm$^{-2}$) and various $q^2$-values (Fig. 5). Both the rise and decay rates were dependent on $q^2$, implying that these kinetics represent the diffusion process, i.e., $D$ of the reactant and a product (or an intermediate) are different. Since the sign of the rise and decay components are positive and negative, respectively, the rise represents the diffusion of the product and the decay is the reactant, that is, the photoproduct diffuses faster than the reactant.

The signal intensity was weak at faster observation times, and became stronger with increasing time by decreasing $q^2$. This time dependence indicates the time development of $D$ in the observation time window (100 ms–2 s). To more clearly illustrate the time dependence, the TG signals were plotted against $q^2t$ (Fig. 6). If reaction kinetics are negligible, the time profile is expressed by a combination of the terms of $\exp(-Dq^2t)$ so that the signals plotted against $q^2t$ should be identical[23]. However, the observed profiles are strongly dependent on $q^2$, especially for the signals at larger $q^2$-values. Thus, the TG signals were analyzed based on the time-dependent $D$ model as follows.

$$\mathrm{R} \xrightarrow{h\nu} \mathrm{I}_1 \xrightarrow{k_1} \mathrm{I}_2 \xrightarrow{k_2} \mathrm{P}, \qquad \text{(Reaction 2)}$$

where R is the reactant PixD decamer, $\mathrm{I}_1$ is the first red-shifted intermediate, $\mathrm{I}_2$ is the

volume-contracted intermediate, P is a photoproduct, $k_1$ is the rate constant of volume contraction ((45 ms)$^{-1}$), and $k_2$ is the rate constant of the *D*-change. Here, we included the volume change reaction ($k_1$ step), because the volume grating component was observed even under the strong excitation conditions employed, although it was much weaker than the diffusion signal which is not visible in the figure. According to the scheme of the Reaction 2, by solving the diffusion equation coupled with the above reaction, an analyzing equation after the thermal grating was derived as:

$$\begin{aligned} I_{\mathrm{TG}}(t) = \alpha\Big[ & -\delta n_{\mathrm{R}}^{0} \exp(-D_{\mathrm{R}} q^2 t) \\ & + \left\{ \delta n_{\mathrm{I}_1}^{0} - \delta n_{\mathrm{I}_2}^{0} \frac{k_1}{k_1 - k_2} + \delta n_{\mathrm{P}}^{0} \frac{k_1 k_2}{k_1 - k_2} \frac{1}{(D_{\mathrm{I}_1} - D_{\mathrm{P}}) q^2 + k_1} \right\} \exp\{-(D_{\mathrm{I}_1} q^2 + k_1) t\} \\ & + \left\{ \delta n_{\mathrm{I}_2}^{0} \frac{k_1}{k_1 - k_2} - \delta n_{\mathrm{P}}^{0} \frac{k_1 k_2}{k_1 - k_2} \frac{1}{(D_{\mathrm{I}_2} - D_{\mathrm{P}}) q^2 + k_2} \right\} \exp\{-(D_{\mathrm{I}_2} q^2 + k_2) t\} \\ & + \delta n_{\mathrm{P}}^{0} \frac{k_1 k_2}{k_1 - k_2} \left\{ \frac{1}{(D_{\mathrm{I}_2} - D_{\mathrm{P}}) q^2 + k_2} - \frac{1}{(D_{\mathrm{I}_1} - D_{\mathrm{P}}) q^2 + k_1} \right\} \exp(-D_{\mathrm{P}} q^2 t) \Big]^2 \end{aligned} , \tag{5}$$

where $\delta n^0$ and *D* are the initial refractive index change and *D* of each species indicated by subscripts, respectively. This equation appears to be complicated and it seems to contain too many parameters to fit the TG signal uniquely. However, we can reduce the number of parameters as follows. First, *D* of the reactant ($D_{\mathrm{R}}$) should be the same as Reaction 1 (3.7 × 10$^{-11}$ m$^2$ s$^{-1}$). Second, since the time constant of the *D*-change ($k_2^{-1}$) is much slower than that of the volume change of the Reaction 1 (45 ms)$^{-1}$, it is reasonable to assume that the reaction until $\mathrm{R} \xrightarrow{h\nu} \mathrm{I}_1 \xrightarrow{k_1} \mathrm{I}_2$ is the same as the Reaction 1. Although the signal intensity is much weaker than the diffusion signal, the volume change process was detected before the diffusion signal, and the time constant and the magnitude is similar to that of the TG signal for the Reaction 1. Hence, $D_{\mathrm{I}_1}$ and $D_{\mathrm{I}_2}$ should be 3.7 × 10$^{-11}$ m$^2$ s$^{-1}$, and $k_1$ should be (45 ms)$^{-1}$. Third, we found that the *D*-change dynamics is over in the time range of the diffusion signal at the smallest $q^2$-value (2 s–10 s). Hence, we can neglect the time dependence of *D* in this time range and the signal should be reproduced by a simple double exponential function:

$$I_{\mathrm{TG}}(t) = \alpha\left\{\delta n_{\mathrm{P}}^{0} \exp(-D_{\mathrm{P}} q^2 t) - \delta n_{\mathrm{R}}^{0} \exp(-D_{\mathrm{R}} q^2 t)\right\}^2 . \tag{6}$$

This fitting is rather simple and there is no ambiguity in determining $D_{\mathrm{P}}$; which was determined to be (7.5 ± 0.5) × 10$^{-11}$ m$^2$ s$^{-1}$. By using these pre-determined values, only $k_2$ was an adjustable parameter to reproduce the signal. Based on the global analysis using Eq. (5), the signals were perfectly reproduced and the time constant of the *D*-change was determined

to be (350 ± 100) ms. The scheme and the determined values are reasonable, because the TG signals at any laser power was reproduced well by the combination of Eqs. (2) and (5).

We found above that the photoproduct has a larger *D*-value than the reactant. An important question which arises is; what is the product? The determined *D*-value represents a clear clue. The *D*-value of the product, $7.5 \times 10^{-11}$ $m^2$ $s^{-1}$, is close to that of calculated molecular mass of the PixD dimer (36 kDa). Therefore, the Reaction 2 represents the light-induced dissociation reaction of the PixD decamer to the dimer. This assignment was independently confirmed by size exclusion chromatography, as described below.

The observation that the signal depends on the excitation laser power indicates that multi-photon or multi-excitation processes is involved in this reaction. There are two possibilities for a multi-photon excitation of an oligomeric protein; one protein absorbs some photons simultaneously or some proteins are excited within a laser pulse. We excluded the former possibility by the repetition rate dependence of the excitation pulses as follows. When we used the weak laser power of 0.2 mJ $cm^{-2}$ at a low repetition rate (< 0.03 Hz), we observed the TG signal of the Reaction 1 (Fig. 1). However, when we excited the sample at the same laser power with a repetition rate of 1 Hz, which is much shorter than the lifetime of the red-shifted species, the single rise–decay signal (Reaction 1) was detected by the first pulse, and then the signal shape gradually changed by successive irradiation, and finally the signal corresponding to the Reaction 2 was observed. This observation strongly suggests that the dissociation reaction of the PixD decamer occurs under multiple-excitation of two individual subunits in the PixD decamer, but not a two-photon excitation of one subunit.

The number of the photoexcited units that are necessary for this reaction was estimated as follows. For a dominant dissociation reaction (Reaction 2), the light intensity of > 10 mJ $cm^{-2}$, which corresponds to a photon density of 200 μM, is required. Taking into account the absorbance (0.5) and reaction quantum yield (0.3), we estimated the concentration of the red-shifted intermediate under the present experimental conditions as ca. 30 μM. This number is approximately twice the concentration of the PixD decamer used (less than 17.3 μM; protein concentration of the monomer unit was 173 μM). Therefore, roughly speaking, we need photo-activation of two chromophores in the decamer for inducing this reaction. (Since the distribution of the number of the excited unit is always unavoidable, there should not be clear threshold for this effect. However, a qualitative consideration (the TG signal intensity of Reaction 2 relative to that of Reaction 1 decreased with decreasing the excitation light intensity below 10 mJ/$cm^2$, which corresponds to the photo-activation of two chromophores in the decamer) clearly suggested that more than 2 excited units are necessary for the

dissociation reaction. A more quantitative and precise analysis of the laser power dependence was difficult, because the absolute signal intensities of Reaction 1 and Reaction 2 could not be determined separately.)

Do the dissociated dimers recover to the decamer during the dark adaptation and what is the kinetics of the recombination of the dimer to the decamer? To answer these questions, we performed a recovery experiment using the TG method. When the sample solution was continuously irradiated by blue light, all PixD exist as the dimer. Under this condition, the diffusion signal derived from the PixD decamer was not observed. In contrast, after terminating the light irradiation, the signal intensity recovered to the original level gradually (dotted trace in Fig. 8). In this case, since the contribution of $\delta n_1(t)$ is negligible, the signal intensity may be expressed as:

$$I_{\mathrm{TG}}(t) = \alpha\left\{f_d(t')\delta n_2(t)\right\}^2, \qquad (7)$$

where *t'* and *t* represent time after terminating the pre-irradiation and after the TG excitation, respectively. Since the signal intensity should be defined by the number of the recombined PixD decamers, the recombination rate can be roughly estimated from the time dependence of $f_d$ as $f_d(t') = \exp(-k_{rec}t')$. The recovering rate constant, $k_{rec}$, was determined to be (~13 s)$^{-1}$, which is very similar to the spectral recovery rate of the red-shifted species[3]. Hence, the light-induced dissociation of the PixD decamer is a transient reaction, and the recombination of the PixD dimers to decamers could be coupled with the ground state recovery of the hydrogen bond network in the vicinity of the chromophore.

**Oligomeric states of PixD in solution**

The results of the TG measurements suggest that PixD exists as a decamer in the dark and when excited with strong light it dissociates into the dimer. In order to confirm such an oligomeric state and the light-induced change, we preformed additional experiments, SEC and BN-PAGE measurements. First, the molecular mass in the dark was measured by the SEC method. The elution profile of PixD in the dark state (continuous curve in Fig. 7(A)) showed double peaks at molecular masses of 187 and 34.2 kDa (Fig. 7(C)), corresponding to the decamer and dimer of PixD, respectively. Even at a lower concentration, the PixD decamer in solution in the dark was observed (dotted curve in Fig. 7(A)). Furthermore, the proteins were separated by BN-PAGE method. The decamer and dimer (or higher oligomer) of PixD were observed as shown in (Fig.7(A) inset). These results indicate that decamer and dimer indeed coexist in solution and both species are excited in the TG measurement. It should be noted, however, that only the decamer as the reactant was observed in the TG signal. Therefore, we

concluded that only the decamer, not the dimer, is photo-responsible to exhibit the TG signal. This conclusion is consistent with the fact that the TG signal was not observed under the continuous light-irradiated condition.

PixD has been reported to form a decamer composed of two-stacked pentameric rings in the crystal. Although oligomeric states of PixD in solution have been reported by means of similar chromatographic methods, including the presence of dimer, trimer, or tetramer[3,7,10], the existence of solely the decamer form of PixD in solution was demonstrated in this experiment for the first time. The exact origin of the difference is not known at present and the origin should be examined in future. However, a possible explanation for the formation of the decamer may be that our construct in this study was essentially the intact form of the protein (plus one amino acid from the expression vector at the N-terminus) compared to ones in previous reports (three additional residues). The difference originated from the two residues extension could affect the decamer formation, possibly due to steric hindrance. In fact, only the dimer form was observed for the N-terminal His-tagged PixD (20 extra residues at N-terminus)[3].

Since the ratio of the elution peak intensity was dependent on the protein concentration (Fig. 7(A)), these oligomers may be in equilibrium in the dark state. However, the double peak in the elution profile indicates that the equilibrium between the decamer and dimer should be slower than 15 min (If equilibrium is faster than the chromatographic running, a single peak at an apparent molecular weight between two oligomeric states would be observed).

The elution profile was next characterized under the light-illuminated condition (dashed curve in Fig. 7(B)). Interestingly, the elution peak of the PixD decamer completely disappeared upon light irradiation with a simultaneous enhancement in the intensity of the dimer peak. This result clearly indicates the light-induced dissociation of the PixD decamer to the dimer. However, since the SEC experiment was carried out under continuous illumination during the elution process with a high power lamp, the kinetics of the dissociation reaction could not be determined, and it is not apparent from this SEC measurement if this dissociation is induced by the excitation of single unit or multiple units. The TG measurement provides a more detailed reaction scheme as shown in the above sections.

**M93A mutant of PixD**

To gain further insight into the molecular mechanism of the light-induced conformational dynamics of PixD, we investigated the photoreaction of the M93A-mutated

PixD by the TG method. A conserved Met residue among all BLUF proteins (Met93 in the case of PixD) is located on the β5-strand of the BLUF domain, which represents the interfacing space between subunits in the crystallographic decamer[5]. Furthermore, the Met93 residue was reported to be crucial for light signal transduction of PixD in *in vitro* and *in vivo*, since site-directed mutagenesis of the Met93 to Ala inhibited the light-dependent interaction change with PixE and the M93A PixD-complemented *Synechocystis* strain as well as the *pixD*-deletion mutant showed negative phototaxis contrary to the observed positive phototaxis of the wild-type strain[22]. Thus, Masuda *et al.* proposed that the PixD M93A mutant may be biochemically and functionally compatible with the light-adapted state of the wild-type (WT) PixD[22]. The Met93 residue appears to form a hydrogen bond with Gln50 in the dark state, and the hydrogen bond is disrupted in the light state. Therefore, the mutation of the Met93 could also induce a structural change even in the dark state. Signal transduction is lost due to the mutation, despite the fact that the absorption spectroscopy showed that the M93A mutant protein retains the normal red-shifting photoreaction[5].

Fig. 9 depicts the TG signal of the M93A mutant with that of the WT PixD measured under the same experimental conditions. The TG signal which reflects the volume change and the *D*-change was almost absent for the M93A mutant. (Hence, the D value of the reactant could not be determined.) This result is consistent with the results of the light-induced FTIR difference spectroscopy of WT and M93A PixD proteins[22]. In the FTIR difference spectra, WT PixD showed a change in the amide II region that was assigned to changes in the structure of the protein backbone, whereas the M93A mutant did not show any change in this region upon photoexcitation. Thus, we assigned the volume contraction with the time constant of 45 ms to a conformational change of the Met93 residue. As revealed by crystallographic, FTIR and fluorescence studies[5,22], the β5-strand containing the Met93, and also a highly conserved Trp91, undergoes a significant conformational change upon excitation. Since the β5-strand and the adjacent loop region represent the major part of the interface between subunits in the PixD decamer, the conformational change of this region could reduce the interprotein interaction, and eventually induce the dissociation of the decamer.

The SEC data of the M93A mutant showed only a single peak, with the elution volume of this peak equal to a species with a mass of 33 kDa; which is in good agreement with the calculated mass of the dimer (Fig. 10). This result suggests that the stabilization of the PixD decamer arises from interprotein interactions around the Met93 residue. From this point, we speculate that the structure around the β5-strand of the M93A mutant may adopt the light state conformation of the WT protein, thereby destabilizing the decamer. This idea supports the

absence of the interaction between PixE and the M93A mutant in both the dark and light states[22]. If the conformation of the Met93 was locked in the WT-light-like state to decouple signal transduction, the transient conformational fluctuation of the interface region may be important for controlling the light information transfer pathway.

It may be instructive to point out that this M93A mutant is biologically inactive; however, it produces the red-shifted species. In some cases, the activity of photoreceptor proteins is examined by the absorption spectral changes upon light illumination. However, this mutant shows that this absorption measurement may provide only a particular condition and is not a sufficient approach to show biological activity. On the other hand, the diffusion signal detected by the TG method correctly predicts the biological activity regardless of the absorption change. We consider that this observation reflects that biological function is induced by large scale motion of the protein system.

**Dissociation reaction of PixD**

There could be two possible forms for the PixD dimer; one is a dimer formed by neighboring subunits in the same pentameric ring (“lateral” with respect to the interfacing plane between the rings; *L*-type), and the other form is one involving monomeric units from the different rings (“vertical”; *V*-type). It is very difficult to experimentally determine which dimer is formed following photoexcitation. However, we consider that the M93A dimer is the *V*-type dimer as follows. The Met93 residue is located within the interfacing part between the *L*-type dimerization site. From the experiments using the M93A mutant, it was shown that the absence of the Met93 enhances the dimer contribution, suggesting that the dimer of M93A is the *V*-type dimer. As stated above, the dimer of M93A presumably corresponds to the light-activated state of WT PixD (the photodissociated dimer). Hence, we conclude that the dimers of WT PixD are also the *V*-type dimer. This assignment is consistent with the suggestion of the *V*-type PixD dimer by Yuan and Bauer based on dissociation free energy calculations and the complexation significance scores[7]. Furthermore, the crystal structures of other BLUF proteins, namely BlrB[27] and the AppA BLUF domain[17,18] show a similar arrangement to the putative *V*-type PixD dimer. Hence, it is highly plausible that the PixD decamer is photodissociated to generate five pairs of the *V*-type PixD dimer that can be stabilized by the interaction between β-sheets of the BLUF domain.

We propose that the decamer formation of PixD helps in the association with PixE, because the M93A protein, which could not form the decamer, lacks the ability to interact with PixE. Although Yuan and Bauer showed that PixD exists as a stable dimer in solution

and the presence of PixE drives the formation of the PixD decamer ($PixD_{10}$–$PixE_5$ complex formation), they did not observe the PixD decamer[7]. It is possible to explain the formation of the complex using an excluded volume effect of the external PixE (the crowding effect). In fact, the decamer formation is accelerated under crowded conditions in the case of TePixD, which is in equilibrium between a decamer and a pentamer in the dark state[28]. We conclude that the decamer formation of the PixD protein and the conformational change of the dimer–dimer interface in the decamer, particularly the conserved Met93 residue, are important for controlling downstream signal transduction for the physiological function of PixD.

The observation of the dissociation reaction of the PixD decamer without PixE provides insights into the PixD-PixE interaction. Currently, it is speculated that the biological function of PixE is suppressed in the bound form and the release of PixE from the complex by the disassembly of the PixD decamer generates a biological output signal[7]. Therefore, the dissociation reaction of PixD observed in this study could be a template for the PixD-PixE interaction. More direct information on the protein–protein interaction between PixD and PixE should be investigated.

## Conclusions

The light-induced reaction dynamics of the BLUF photoreceptor *Synechocystis* PixD was studied using time-resolved TG and chromatographic methods in solution, and combined with site-directed mutagenesis of the conserved Met93 residue. A volume contraction of 13 mL $mol^{-1}$ was observed with a time constant of 45 ms following photoexcitation, and this contraction was attributed to a conformational change around the Met93 residue. The determined *D*-value ($3.7 \times 10^{-11}$ $m^2$ $s^{-1}$) and SEC results clearly showed that PixD forms a decamer in solution in the dark state. The PixD decamer was found to transiently dissociate to a dimer based on the results from the TG and SEC under light-irradiated conditions. The TG method further revealed that this reaction occurs by multiple excitations of two chromophores in the decamer and the time constant was determined as the rate of the *D*-increase (from $3.7 \times 10^{-11}$ to $7.5 \times 10^{-11}$ $m^2$ $s^{-1}$) to be 350 ms. The observation that the PixD M93A mutant lost the ability to form the decamer but formed the dimer indicates that the conformational change at the dimer–dimer interface region in the PixD decamer, particularly the β5-strand and the adjacent loop that contains the Met93 residue, is critical for facilitating light signal transduction of the PixD photoreceptor. Finally, our observations provide important insights into the interprotein interaction between PixD and PixE, which is directly related to the biological function. The study on the protein-protein interaction dynamics by the TG method

with the purified PixD–PixE complex is currently underway, and will be reported in the near future.

## Materials and Methods

### Cloning, expression, and purification

The wild-type PixD sequence was inserted into the pET28a vector, as previously described[3]. Site-directed mutagenesis to generate the M93A PixD mutant was performed using the PCR-based Quick Change site-directed mutagenesis kit (Stratagene) with primers (sense, 5'-GAGGTTTGGTCTGCGCAAGCGATCACG-3'; antisense, 5'-CGTGATCGCTTGCGCAGACCAAACCTC-3'). The plasmid carrying the desired substitution was confirmed using nucleotide sequencing with the BigDye terminator fluorescence detection method (Applied Biosystems) and a capillary sequencer (PRISM 310 Genetic Analyzer, Applied Biosystems).

The wild-type and M93A mutant PixD proteins were expressed in *Escherichia coli* BL21 (DE3). Cells were cultured in LB medium containing 20 μg $ml^{-1}$ kanamycin for 30 h at 25 °C and harvested by centrifugation at 4,000 *g* for 15 min at 4 °C. Freeze-thawed cells were suspended in a buffer containing 20 mM Hepes-NaOH (pH 7.5) and 500 mM NaCl. After disruption of the cells by sonication, the homogenate was centrifuged at 75,000 *g* for 30 min at 4 °C. The His-tagged fusion protein was purified from the supernatant by Ni-affinity column chromatography (GE Healthcare, HisTrap FF). After the medium was exchanged to a 20 mM Tris-HCl (pH 7.5) buffer containing 500 mM NaCl using a desalting column, the N-terminal His-tag was cleaved off by 500 units of thrombin protease (GE Healthcare) per 4 mg protein for 6 h at 20 °C. Benzamidine sepharose (GE Healthcare) was added to the solution to remove thrombin, and then, the cleaved His-tag polypeptide and the uncleaved fusion protein were trapped by passing over the Ni-column. The flow through from the column was pooled and concentrated as a final purified sample solution. The appropriate cleavage and purity of >95% were confirmed by sodium dodecyl sulfate polyacrylamide gel electrophoresis (SDS-PAGE). The protein concentration was determined by a method based on the protocol described in ref 29. Briefly, flavin was extracted from the protein by SDS-treatment, and absorption spectrum was measured. According to the absorption peak position corresponding to the $S_1 \leftarrow S_0$ transition and the previous TLC result[3], our sample prepared by the above procedure contained FAD as a chromophore and other possible contributions (such as FMN) are negligible. Moreover, the absorption spectrum of the protein solution indicated that our sample binds the chromophore with the stoichiometric amount[3].

The protein concentration was measured by the absorbance at 473 nm. At this wavelength, the extinction coefficient of FAD and FMN is the same (9200 $M^{-1}$ $cm^{-1}$) [29]. The concentration of the PixD proteins used in this study was 173 μM.

**Transient grating (TG)**

TG measurements were performed using a similar setup previously reported[6,20–23,25]. Usually, 20–100 signals were averaged by a digital oscilloscope (Tektronix, TDS-7104) to improve the signal-to-noise ratio. The repetition rate of the excitation was <0.03 Hz to avoid photoexcitation of a photoproduct. At higher laser power excitations, a single shot-signal acquisition procedure was also used. The sample solution was stirred after every shot to refresh the sample in the excited volume. The $q^2$-value was determined from the decay rate of the thermal diffusion signal of bromocresol purple in water (a calorimetric reference). For quantitative measurement of $\Delta V$, absorbance of the reference and sample solutions was prepared to be identical at the excitation wavelength. The excitation laser power was changed by adjusting the amplifier of the dye laser or variable neutral density filters, and monitored by a pyroelectric Joulemeter (Coherent, J3-09).

**Size exclusion chromatography (SEC) and Blue native-polyacrylamide gel electrophoresis (BN-PAGE)**

SEC was conducted with Superdex 200 10/300 GL column (GE Healthcare) equilibrated with a 20 mM Tris-HCl (pH 7.5) buffer containing 500 mM NaCl. Elution profiles were monitored by the absorbance at 280 and 440 nm using an ÄKTA purifier system (GE Healthcare). Dark state measurements were carried out in the dark using the column covered with aluminum foil. For the light state experiments, continuous white light from a Xe lamp (Ushio, Optical Modulex SX-UI500XQ) through a heat-ray absorbing glass was illuminated on the column during the chromatographic experiments. The column was calibrated using a gel filtration calibration kit (GE Healthcare), which included ferritin (440 kDa), aldolase (158 kDa), ovalbumin (43 kDa) and ribonuclease A (13.7 kDa), as molecular weight standards. The apparent molecular mass of elutes from the column was determined from the calibration curve.

BN-PAGE was performed using the NativePAGETM Novex® Bis-Tris Gel system (invitrogen). The sample solution was the same as the SEC experiment.

## Acknowledgments

This work was supported by Grant-in-aid for Scientific Research (No. 18205002) and Grant-in-aid for Scientific Research on Innovative Areas (research in a proposed research area) (20107003) from the Ministry of Education, Culture, Sports, Science and Technology in Japan (to M.T.). K.T. was supported by the Global COE program, Integrated Materials Science, Kyoto University, Japan, and by the Research Fellowships for Young Scientists of the Japan Society for the Promotion of Science.

## References

1. Gomelsky, M. & Klug, G. (2002). BLUF: a novel FAD-binding domain involved in sensory transduction in microorganisms. *Trends Biochem. Sci.* **27**, 497–500.
2. van der Horst, M. A. & Hellingwerf, K. J. (2004). Photoreceptor proteins, “star actors of modern times”: a review of the functional dynamics in the structure of representative members of six different photoreceptor families. *Acc. Chem. Res.* **37**, 13–20.
3. Okajima, K., Yoshihara, S., Fukushima, Y., Geng, X., Katayama, M., Higashi, S. *et al.* (2005). Biochemical and functional characterization of BLUF-type flavin-binding proteins of two species of cyanobacteria. *J. Biochem. (Tokyo)*, **137**, 741–750.
4. Kita, A., Okajima, K., Morimoto, Y., Ikeuchi, M. & Miki, K. (2005). Structure of a cyanobacterial BLUF protein, Tll0078, containing a novel FAD-binding blue light sensor domain. *J. Mol. Biol.* **349**, 1–9.
5. Yuan, H., Anderson, S., Masuda, S., Dragnea, V., Moffat, K. & Bauer, C. E. (2006). Crystal structures of the *Synechocystis* photoreceptor Slr1694 reveal distinct structural states related to signaling. *Biochemistry*, **45**, 12687–12694.
6. Tanaka, K., Nakasone, Y., Okajima, K., Ikeuchi, M., Tokutomi, S. & Terazima, M. (2009). Oligomeric-state-dependent conformational change of the BLUF protein TePixD (Tll0078). *J. Mol. Biol.* **386**, 1290–1300.
7. Yuan, H. & Bauer, C. E. (2008). PixE promotes dark oligomerization of the BLUF photoreceptor PixD. *Proc. Natl Acad. Sci. USA.* **105**. 11715–11719.
8. Fukushima, Y., Okajima, K., Shibata, Y., Ikeuchi, M. & Itoh, S. (2005). Primary intermediate in the photocycle of a blue-light sensory BLUF FAD-protein, Tll0078, of *Thermosynechococcus elongatus* BP-1. *Biochemistry*, **44**, 5149–5158.
9. Okajima, K., Fukushima, Y., Suzuki, H., Kita, A., Ochiai, Y., Katayama, M. *et al.* (2006). Fate determination of the flavin photoreceptions in the cyanobacterial blue light receptor TePixD (Tll0078). *J. Mol. Biol.* **363**, 10–18.
10. Masuda, S., Hasegawa, K., Ishii, A. & Ono, TA. (2004). Light-induced structural changes in a putative blue-light receptor with a novel FAD binding fold sensor of blue-light using FAD (BLUF); Slr1694 of *Synechocystis* sp. PCC6803. *Biochemistry*, **43**, 5304–531.
11. Gauden, M., van Stokkum, I. H., Key, J. M., Lührs, D. C., van Grondelle, R., Hegemann, P. & Kennis, J. T. M. (2006). Hydrogen-bond switching through a radical pair mechanism in a flavin-binding photoreceptor. *Proc. Natl Acad. Sci. USA.* **103**, 10895–10900.
12. Bonetti, C., Mathes, T., van Stokkum, I. H., Mullen, K. M., Groot, M. L., van Grondelle, R. *et al.* (2008). Hydrogen bond switching among flavin and amino acid side chains in the

BLUF photoreceptor observed by ultrafast infrared spectroscopy. *Biophys. J.* **95**, 4790–4802.

13. Fukushima, Y., Okajima, K., Ikeuchi, M. & Itoh, S. (2007). Two intermediate states *I* and *J* trapped at low temperature in the photocycles of two BLUF domain proteins of cyanobacteria *Synechocystis* sp. PCC6803 and *Thermosynechococcus elongatus* BP-1. *Photochem. Photobiol.* **83**, 112–121.
14. Hasegawa, K., Masuda, S. & Ono, TA. (2004). Structural intermediate in the photocycle of a BLUF (sensor of blue light using FAD) protein Slr1694 in a cyanobacterium *Synechocystis* sp. PCC6803. *Biochemistry*, **43**, 14979–14986.
15. Masuda, S., Hasegawa, K. & Ono, TA. (2005). Light-induced structural changes of apoprotein and chromophore in the sensor of blue light using FAD (BLUF) domain of AppA for a signaling state. *Biochemistry*, **44**, 1215–1224.
16. Masuda, S., Hasegawa, K. & Ono, TA. (2005). Tryptophan at position 104 is involved in transforming light signal into changes of β-sheet structure for the signaling state in the BLUF domain of AppA. *Plant Cell Physiol.* **46**, 1894–1901.
17. Anderson, S., Dragnea, V., Masuda, S., Ybe, J., Moffat, K. & Bauer, C. E. (2005). Structure of a novel photoreceptor, the BLUF domain of AppA from *Rhodobacter sphaeroides*. *Biochemistry*, **44**, 7998–8005.
18. Jung, A., Reinstein, J., Domratcheva, T., Shoeman, R. L. & Schlichting, I. (2006). Crystal structures of the AppA BLUF domain photoreceptor provide insights into blue light-mediated signal transduction. *J. Mol. Biol.* **362**, 717–732.
19. Grinstead, J. S., Hsu, S. T., Laan, W., Bonvin, A. M., Hellingwerf, K. J., Boelens, R. *et al.* (2006). The solution structure of the AppA BLUF domain: insight into the mechanism of light-induced signaling. *ChemBioChem*, **7**, 187–193.
20. Grinstead, J. S., Avila-Perez, M., Hellingwerf, K. J., Boelens, R. & Kaptein, R. (2006). Light-induced flipping of a conserved glutamine sidechain and its orientation in the AppA BLUF domain. *J. Am. Chem. Soc.* **128**, 15066–15067.
21. Wu, Q. & Gardner, K. H. (2009). Structure and insight into blue light-induced changes in the BlrP1 BLUF domain. *Biochemistry*, **48**, 2620–2629.
22. Masuda, S., Hasegawa, K., Ohta, H. & Ono, TA. (2008). Crucial role in light signal transduction for the conserved Met93 of the BLUF protein PixD/Slr1694. *Plant Cell Physiol.* **49**, 1600–1606.
23. Terazima, M. & Hirota, N. (1993). Translational diffusion of a transient radical studied by the transient grating method, pyradinyl radical in 2-propanol. *J. Chem. Phys.* **98**,

6257–6262.

24. Terazima, M. (2006). Diffusion coefficients as a monitor of reaction kinetics of biological molecules. *Phys. Chem. Chem. Phys.* **8**, 545–557.
25. Inoue, K., Sasaki, J., Morisaki, M., Tokunaga, F. & Terazima, M. (2004). Time-resolved detection of sensory rhodopsin II-transducer interaction. *Biophys. J.* **87**, 2587–2597.
26. Eitoku, T., Nakasone, Y., Matsuoka, D., Tokutomi, S. & Terazima, M. (2005). Conformational dynamics of phototropin 2 LOV2 domain with the linker upon photoexcitation. *J. Am. Chem. Soc.* **127**, 13238–13244.
27. Jung, A., Domratcheva, T., Tarutina, M., Wu, Q., Ko, W. H., Shoeman, R. L. *et al.* (2005). Structure of a bacterial BLUF photoreceptor: insights into blue light-mediated signal transduction. *Proc. Natl Acad. Sci. USA.* **102**, 12350–12355.
28. Toyooka, T., Tanaka, K., Okajima, K., Ikeuchi, M., Tokutomi, S. & Terazima, M. Macromolecular crowding effects on reactions of TePixD (Tll0078). *Photochem. Photobiol.* in press.
29. Chapman, S. K. & Reid, G. A. eds. (1999). Flavoprotein Protocols. *Methods in Molecular Biology*; 131. Humana Press Inc. Totowa, New Jersey.

## Figure captions

**Fig. 1.** A typical TG signal (dotted line) after photoexcitation of PixD at $q^2 = 4.0 \times 10^{11}$ m$^{-2}$ and a laser power of 0.2 mJ cm$^{-2}$. The best-fitted curve including the thermal grating and a biexponential function (Eq. (2)) is shown by the continuous line.

**Fig. 2.** $q^2$ dependence of the TG signal of PixD (dotted curves) at lower laser powers (< 0.5 mJ cm$^{-2}$). The $q^2$ values were $1.1 \times 10^{12}$, $8.4 \times 10^{11}$, $4.0 \times 10^{11}$, $2.8 \times 10^{11}$ and $4.0 \times 10^{10}$ m$^{-2}$ from left to right. The signals were normalized by the thermal grating intensity of the reference sample measured under the same conditions. The continuous lines represent fitting curves using Eq. (2).

**Fig. 3.** The rate constants of the rise (squares) and decay (circles) components of the TG signal at lower laser powers (< 0.5 mJ cm$^{-2}$) plotted against $q^2$ values. The lines are the least square fits by $D_1q^2 + k$ and $D_1q^2$ for the rise and the decay components, respectively.

**Fig. 4.** TG signals of PixD at various excitation laser intensities at $q^2 = 4.0 \times 10^{11}$ m$^{-2}$. These signals were normalized by the number of excited molecules. The arrows indicate the direction of the increase in the laser power. The laser powers measured were 0.2, 0.6, 1 and 3 mJ cm$^{-2}$.

**Fig. 5.** $q^2$ dependence of the TG signal of PixD (dotted curves) at higher laser powers (> 10 mJ cm$^{-2}$). The $q^2$ values were $2.8 \times 10^{11}$, $1.1\times 10^{11}$, $3.4 \times 10^{10}$, $1.5 \times 10^{10}$ and $7.8 \times 10^{9}$ m$^{-2}$ from left to right. The signals were normalized by the thermal grating intensity of the reference sample measured under the same conditions. The continuous lines represent fitting curves using Eq. (3).

**Fig. 6.** TG signals of Fig. 5 plotted against $q^2t$ to show the time-dependent $D$. The $q^2$-values were $7.8 \times 10^{9}$, $1.5 \times 10^{10}$, $3.4 \times 10^{10}$, $1.1\times 10^{11}$ and $2.8 \times 10^{11}$ m$^{-2}$ from left to right. These signals were normalized at the peak intensity.

**Fig. 7.** SEC of WT PixD with the Superdex 200 10/300 column. (A) Concentration dependence of elution profiles at 130 μM (continuous curve) and 30 μM (dotted curve). (Inset) Protein separation by BN-PAGE with native conformation and oligomeric states. Two

bands were observed and molecular masses were estimated to be ~180 kDa and ~80 kDa, and assigned to the decamer and dimer (or higher oligomer), respectively. (B) Elution profiles under dark (continuous curve) and light (dashed curve) conditions at 130 μM. A PixD solution was divided into two equal aliquots, and they were subjected to each measurement. (C) A standard curve of the column (solid line) obtained by the molecular weight of marker proteins and the elution volumes $V_e$ (filled circles) ($V_o$: void volume, $V_t$: total column volume). The elution peak positions of WT PixD on the standard curve are shown as open squares, and molecular weights were determined to be 187 kDa and 34.2 kDa that are the decamer and dimer of PixD, respectively.

**Fig. 8.** Time evolution of the TG signal intensity after stopping pre-illumination at $t'$ = 0 (dotted trace). The continuous curve indicates a fitting of the recovery rate of the diffusion signal intensity by $f_d(t') = \exp(-k_{rec}t')$. The recovering rate constant, $k_{rec}$, was determined to be (~13 s)$^{-1}$. The dashed line represents the TG signal intensity without light irradiation. The pre-irradiation was performed with ~1 min of blue light supplied by a diode laser with a wavelength of 449 nm (Micro laser systems, Inc.).

**Fig. 9.** TG signals after the thermal grating of M93A (dotted line) with that of WT PixD (continuous line) at $q^2 = 6.1 \times 10^{10}$ m$^{-2}$ and a laser power of 2 mJ cm$^{-2}$.

**Fig. 10.** SEC profiles of the PixD M93A mutant using the Superdex 200 10/300 column monitored at 280 nm (continuous curve) and 440 nm (dotted curve) under dark conditions. A small peak at ~8 mL $V_e$ indicates the presence of an aggregate eluting at the void volume of the column.
(inset) A standard curve of the column (solid line). The elution peak position of M93A PixD on the standard curve is shown as an open square and the molecular mass was determined to be 33 kDa.

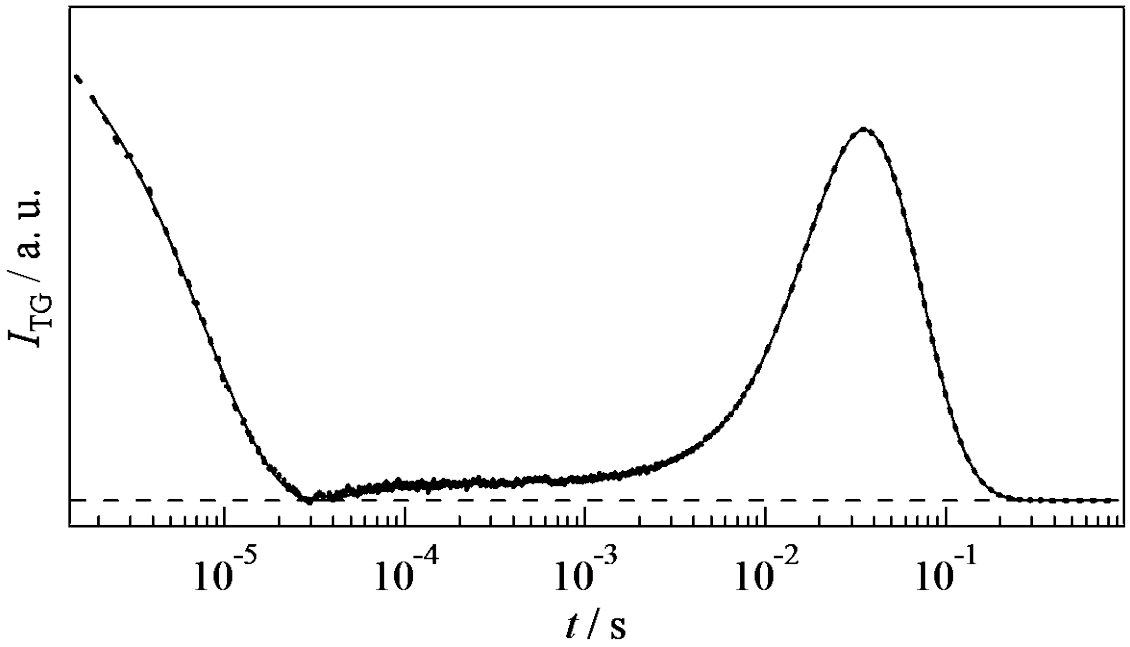


**Fig. 1**

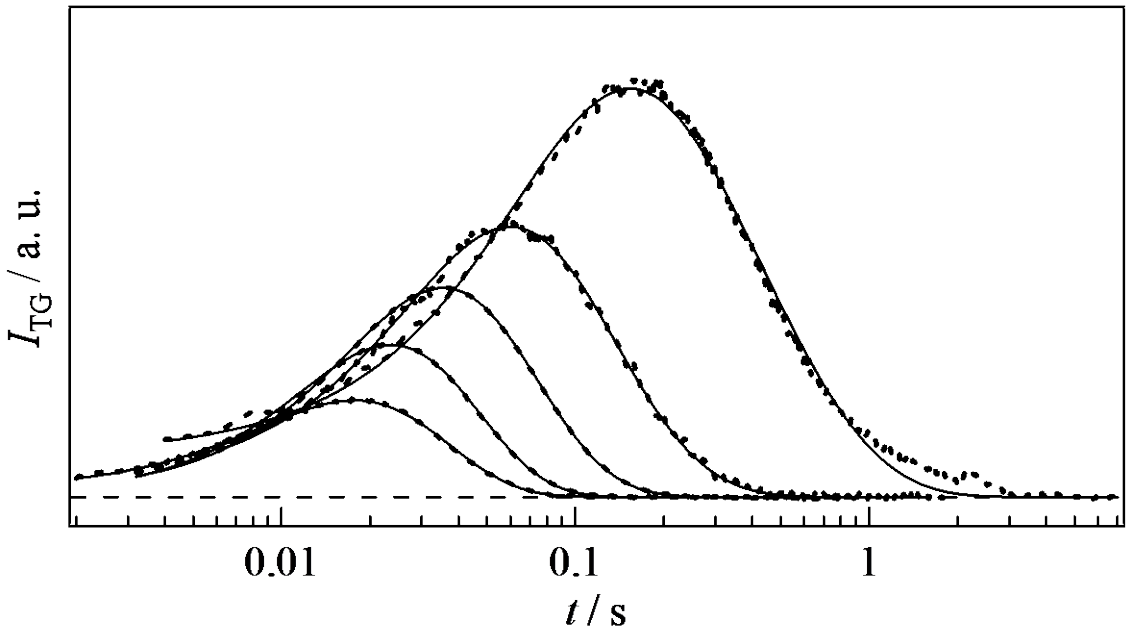


**Fig. 2**

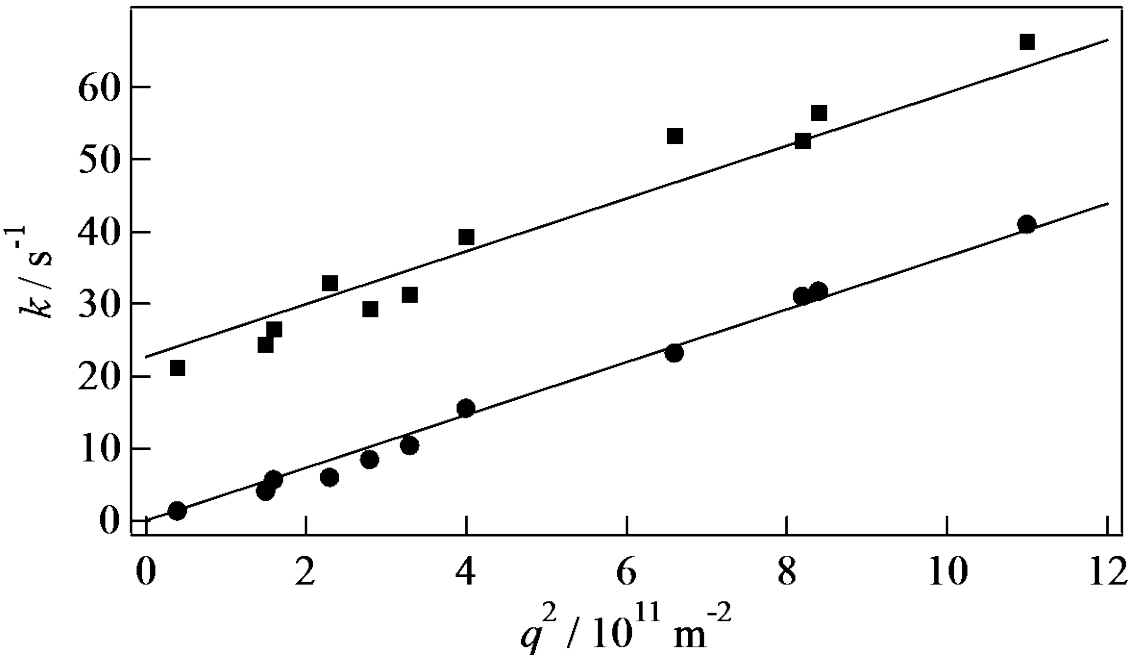


**Fig. 3**

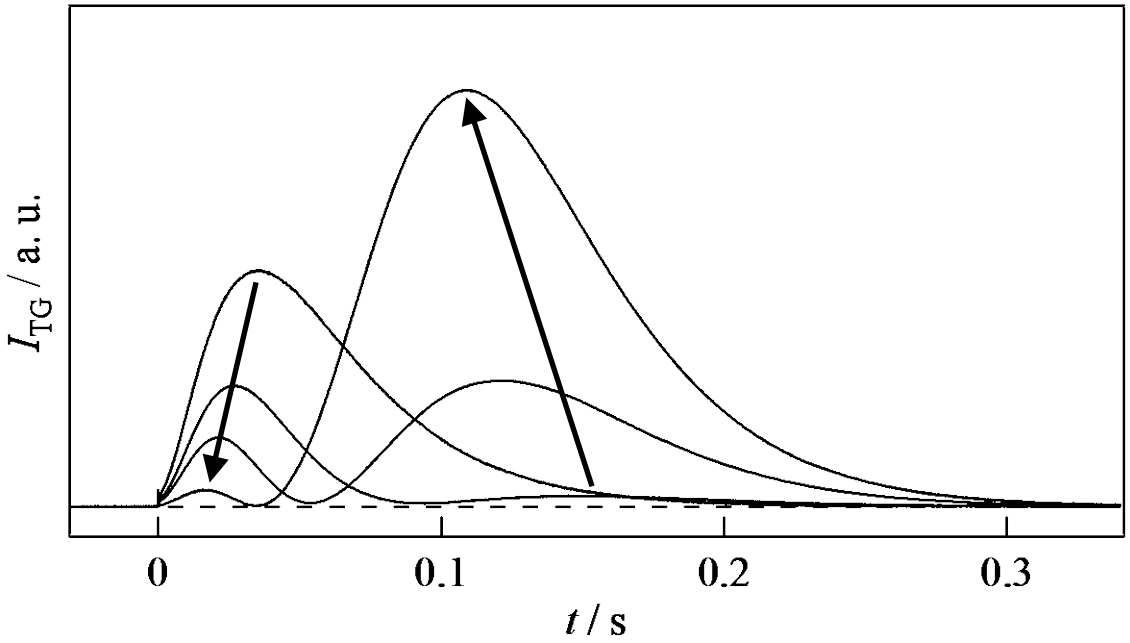


**Fig. 4**

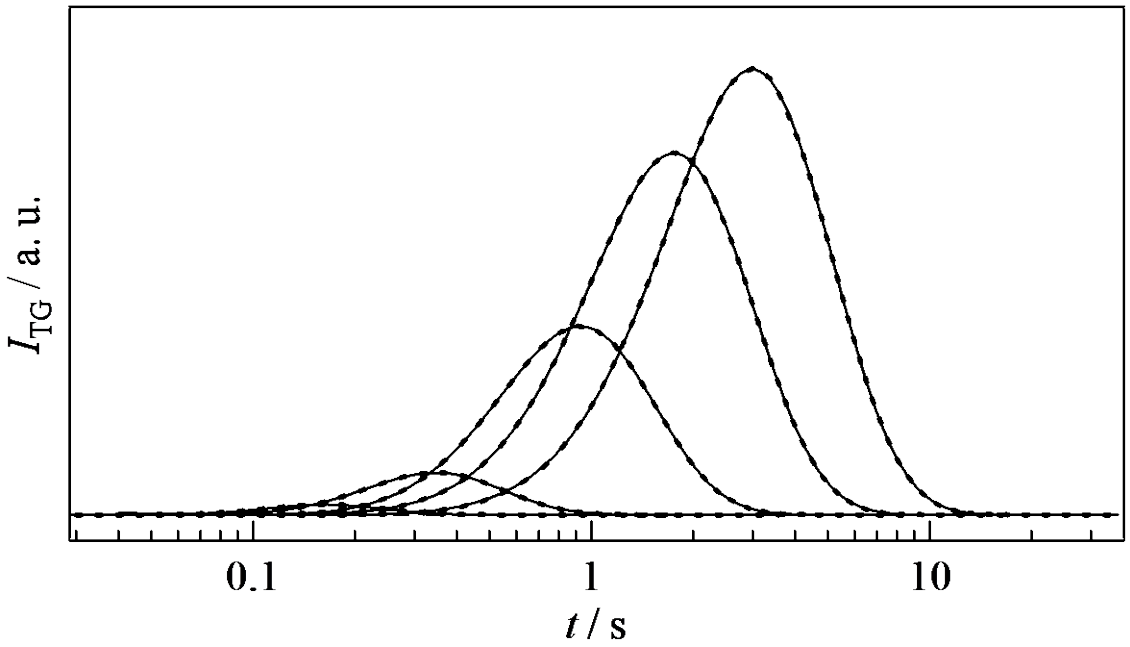


**Fig. 5**

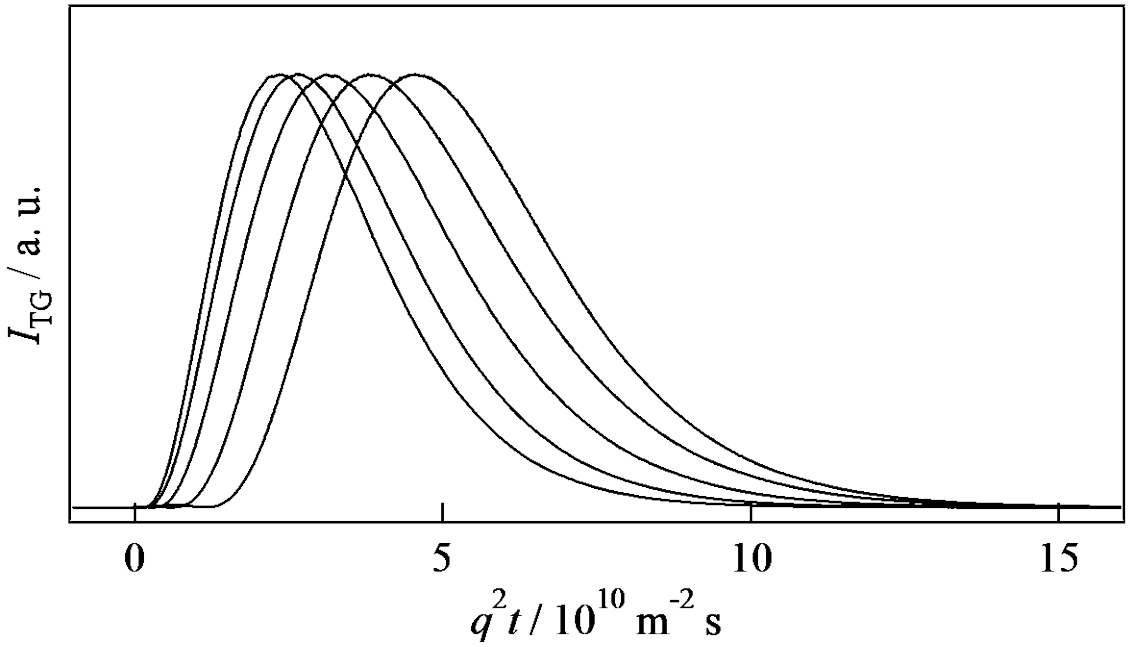


**Fig. 6**

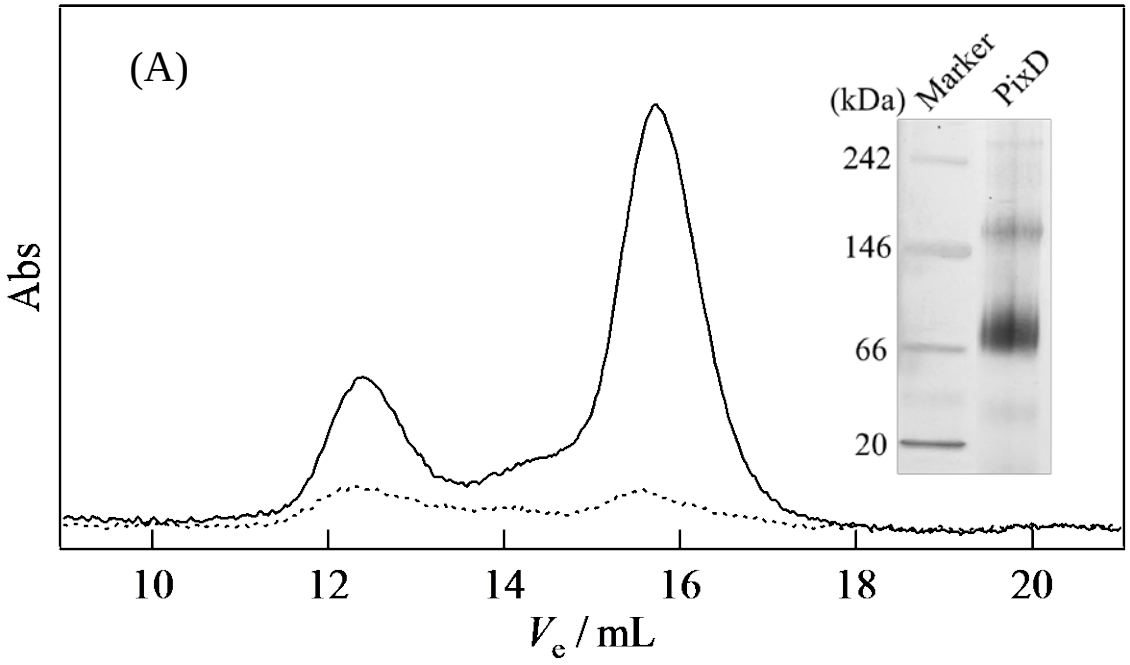


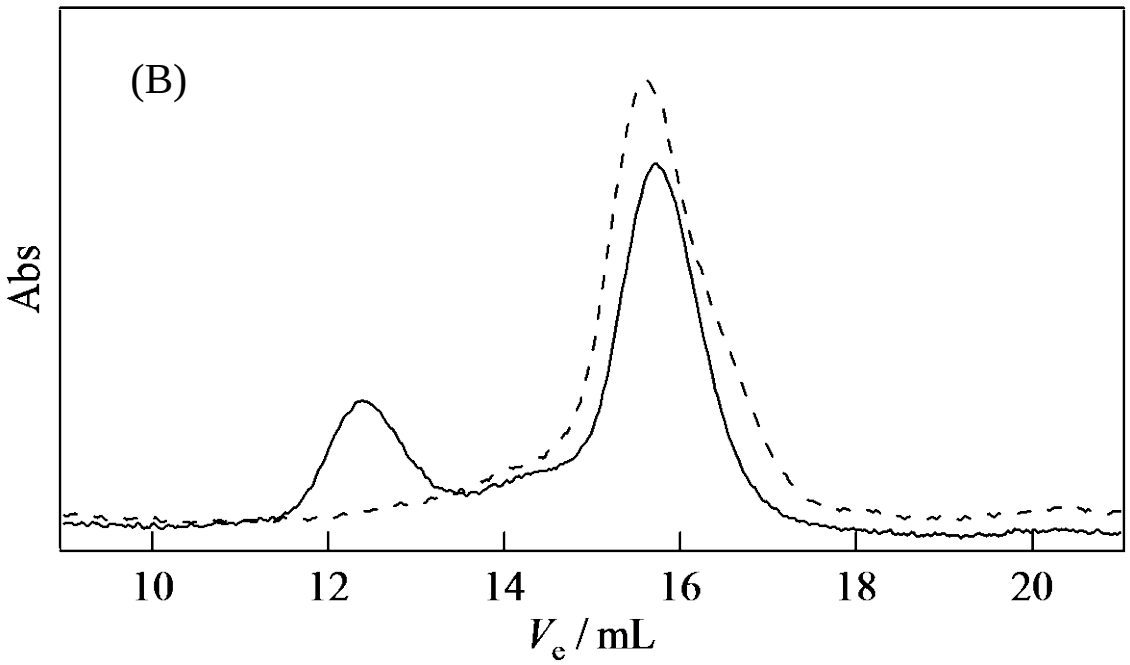

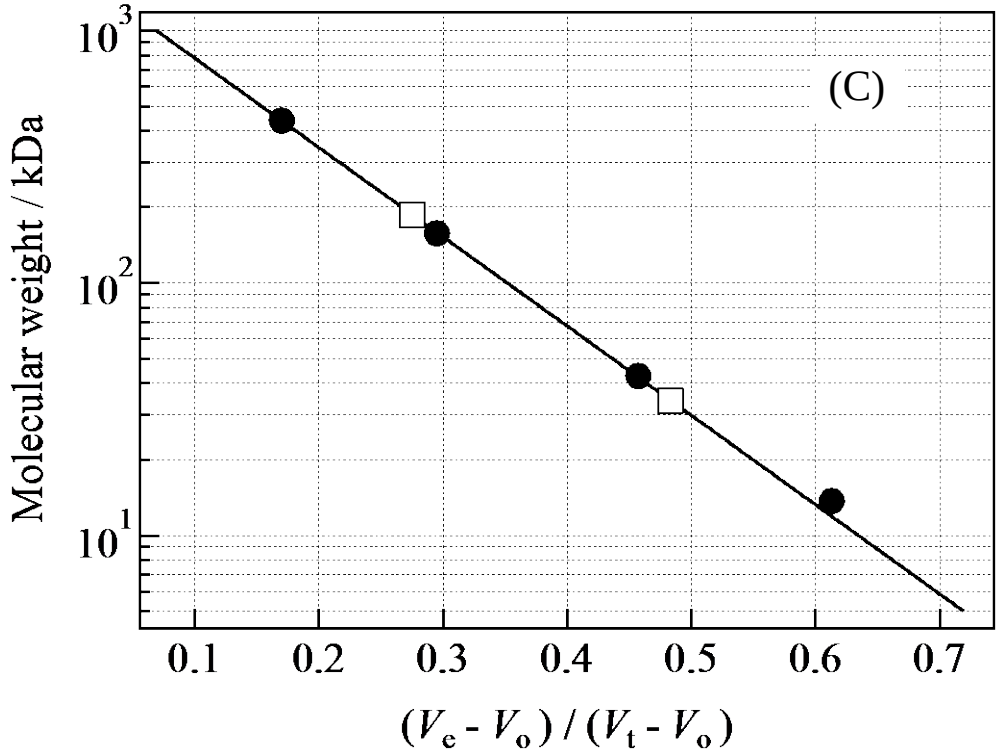


**Fig. 7**

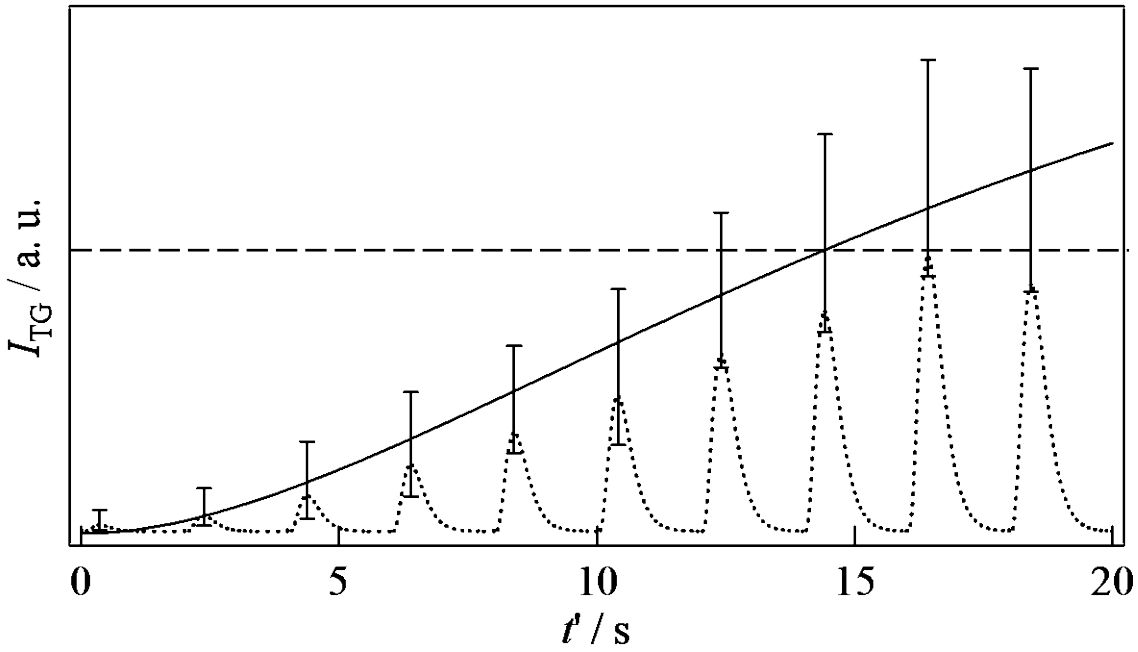


**Fig. 8**

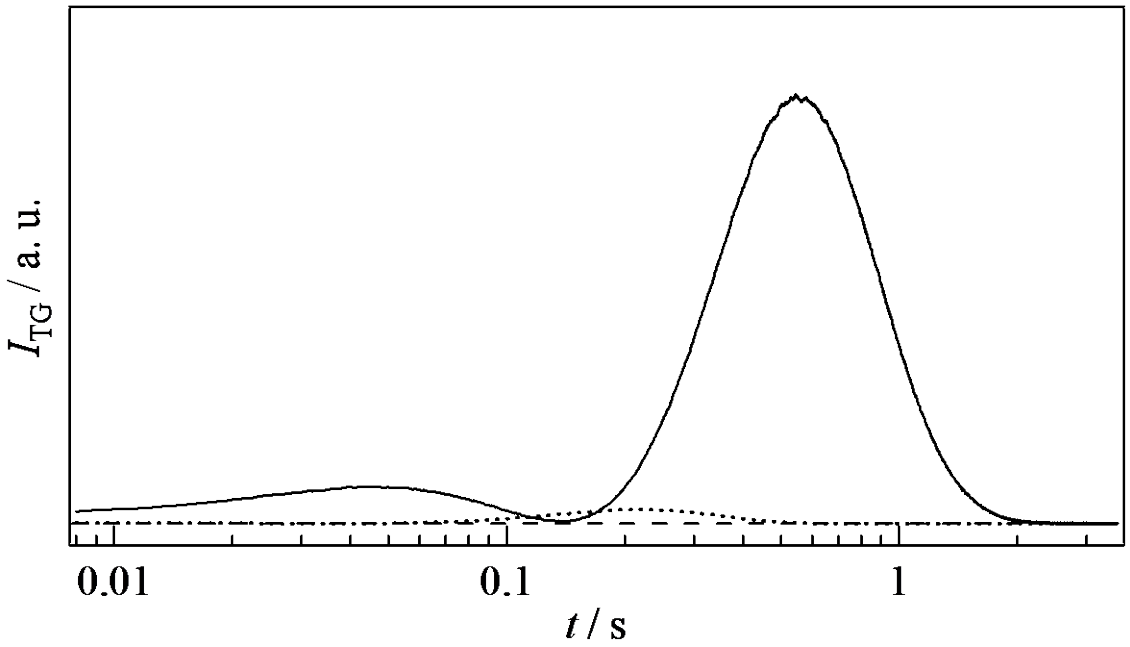


**Fig. 9**

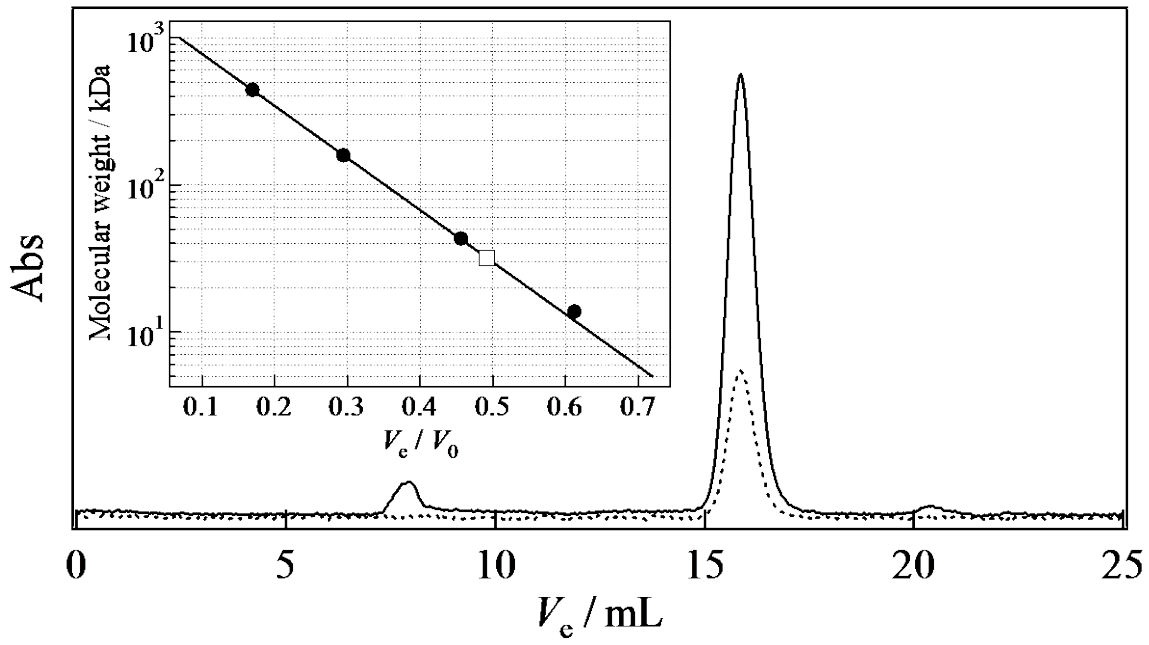


**Fig. 10**

**Graphical abstract**

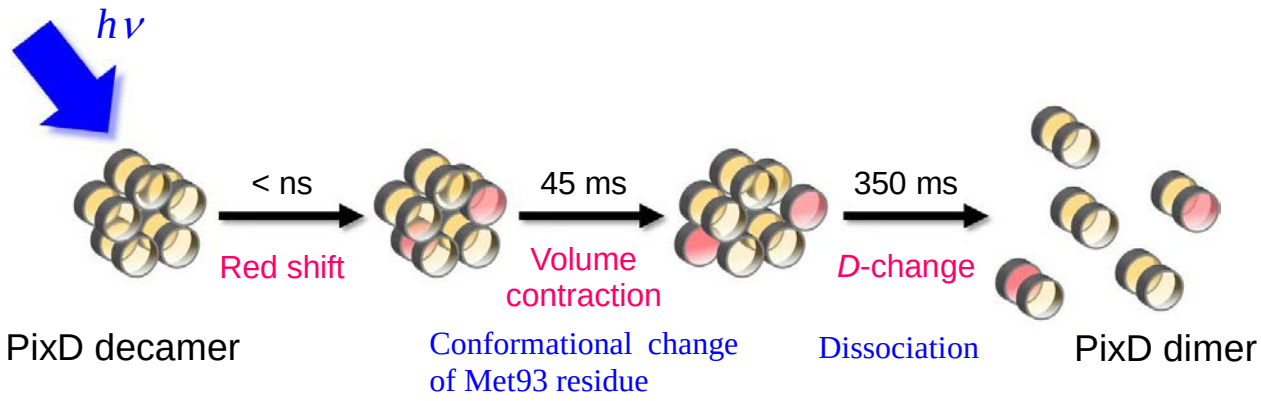


**Research highlights**

PixD forms a decamer in solution. Volume contraction occurs with a time constant of 45 ms, and it was attributed to conformational change of Met93 residue at the interfacing loop structure between subunits. With a strong excitation light, the PixD decamer is dissociated into the dimer with a time constant of 350 ms.